

1

Supporting Information

2

Comprehensive understanding of iron- catalyzed Fischer-Tropsch synthesis product distribution via extensive reliable data

3

4 Kunpeng Song,^{a,b} XiaoFeng Li,^c Wentao Li,^c Xiong Zhou,^c Liping

5 Zhou,^{*c}, Hongwei Xiang,^{a,c}, Yong Yang,^{a,c} and Yongwang Li^{a,c}

6

7 ^aState Key Laboratory of Coal Conversion, Institute of Coal Chemistry,

8 Chinese Academy of Sciences, Taiyuan 030001, PR China

9 ^bUniversity of Chinese Academy of Sciences, Beijing 100049, PR China

10 ^c National Energy Center for Coal to Liquids, Synfuels China Technology

11 Co., Ltd., Huairou District, Beijing 101400, PR China

12

13 Correspondence: Liping Zhou, National Energy Center for Coal to

14 Liquids, Synfuels China Technology Co., Ltd., Huairou District, Beijing

15 101400, PR China. Email: zhouliping@synfuelschina.com.cn

16

17

18 **S1 Details of the mechanism model involved in Fig. 1b of the article**

19 **S1.1 Schulz-Flory model in Fig. 1b1**

20 Schulz-Flory model is applied in Fig. 1b1. This distribution function is used to
21 describe the polymerization process, assuming that all surface oligomers are equally
22 reactive to chain growth and that the rate of carbon-carbon bond formation and product
23 desorption are constant. As shown in Eq. S1.1, this model predicts the linear
24 relationship between $\ln (W_n/n)$ and n , where W_n is the weight fraction of product of
25 carbon number n , and α expresses a probability of addition to the monomer or other
26 surface chains^[1].

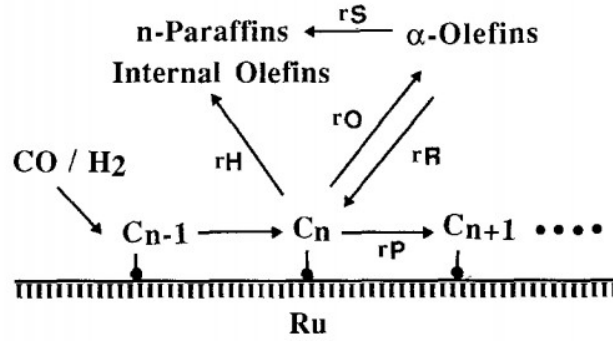
$$27 \quad \ln \frac{W_n}{n} = \ln \frac{(1-\alpha)^2}{\alpha} + n \cdot \ln \alpha \quad (S1.1)$$

28

29 **S1.2 Single-mechanism with diffusion correction in Fig. 1b2**

30 This study uses a diffusion-enhanced α -olefin re-adsorption model^[2]. In the chain
31 growth kinetic model, as shown in Fig. S1-1, surface reaction rate constants are
32 assumed to be independent of chain length for C2+ surface chains. Re-adsorption rate
33 constants are assumed to be independent of chain length for C3+ α -olefins, higher for
34 ethylene, and zero for non-terminal olefin species and for paraffins; thus, any carbon
35 number effects on α or on product functionality arise exclusively from physical
36 transport rather than chemical effects.

37



38

39

Fig. S1-1 Hydrocarbon synthesis chain growth kinetic scheme

40 The steady-state conservation of the catalytic surface chain growth site can be
 41 expressed as,

$$42 \quad -k_p C_1^* C_n^* + k_p C_1^* C_{n-1}^* - k_o C_n^* - k_h C_n^* + k_r P_n^v / RT = 0 \quad (S1.2)$$

43 C^* is the surface coverage of adsorbed species, and P_n^v is the Olefin virtual pressure
 44 in liquid phase. The steady-state conservation between diffusion and reaction can be
 45 expressed as

$$46 \quad \text{Olefin: } D_n \nabla P_n^v - \rho_p [(k_r + k_s) P_n^v - k_o C_n^*] = 0 \quad (S1.3)$$

$$47 \quad \text{Paraffin: } D_n \nabla Q_n^v + \rho_p [k_s P_n^v + k_h C_n^*] = 0 \quad (S1.4)$$

48 Where, D_n is the hydrocarbon diffusivities in liquid filled pores. ρ_p is catalyst pellet
 49 density. Q_n^v is the paraffin virtual pressure in liquid phase.

50 In the transport-enhanced re-adsorption model, the carbon number-dependent olefin
 51 diffusivity is,

$$52 \quad D_n = D_{n,0} e^{-0.3n} \quad (S1.5)$$

53

54 **S1.3 Single-mechanism with solubility correction in Fig. 1b3**

55 This study was carried out in stirred tank slurry reactor using a kinetic model with
 56 solubility enhanced 1-olefin re-adsorption term^[3]. The mechanism is the addition of 2-

57 olefin formation based on the Van der Laan and Beenackers model^[4], as shown in Table
 58 S1-1.

59 **Table S1-1** Elementary steps of hydrocarbon formation

Number	Step	rate equation
HC1	Initiation – formation of adsorbed methyl species $CH_2-s + H-s \leftrightarrow CH_3-s + s$	$r_i = k_i \theta_{CH_2-s} \theta_{H-s}$
HC2	Propagation: $C_n H_{2n+1}-s + CH_2-s \rightarrow C_{n+1} H_{2n+3}-s + s \quad n = 1, 2, 3 \dots$	$r_p^n = k_p \theta_{CH_2-s} \theta_{C_n H_{2n+1}-s}$
HC3	Primary termination to n-paraffin (hydrogenation) $CH_3(CH_2)_n-s + H-s \rightarrow C_n H_{2n+2} + 2s \quad n = 1, 2, 3 \dots$	$r_{t,p}^n = k_{t,p} \theta_{H-s} \theta_{C_n H_{2n+1}-s}$
HC4	Primary termination to 1-olefin (dehydrogenation and desorption) $C_n H_{2n+1} s + s \rightarrow C_n H_{2n} + H-s + s \quad n = 2, 3 \dots$	$r_{t,1o}^n = k_{t,1o} \theta_s \theta_{C_n H_{2n+1}-s}$
HC5	1-olefin re-adsorption on primary sites $C_n H_{2n} + H-s + s \rightarrow C_n H_{2n+1}-s + s \quad n = 2, 3 \dots$	$r_{r,1o}^n = k_{r,1o} \theta_s \theta_{H-s} C_{1-C_n H_{2n}}^s$
HC6	Primary termination to 2-olefin (dehydrogenation and desorption) $C_n H_{2n+1} s + s \rightarrow 2-C_n H_{2n} + H-s + s \quad n = 4, 5 \dots$	$r_{t,2o}^n = k_{t,2o} \theta_s \theta_{C_n H_{2n+1}-s}$

60 Reaction equations of methane, ethylene, n-paraffin and 1-olefin can be written as:

61
$$R_{CH_4} = \kappa_{t,p}^{(1)} \frac{\kappa_1}{\kappa_p + \kappa_{t,p}^{(1)}} \quad (S1.6)$$

62
$$R_{C_2H_6} = \kappa_{t,p}^{(2)} \frac{\kappa_1}{\kappa_p + \kappa_{t,p}^{(1)}} \alpha_2 \quad (S1.7)$$

63
$$R_{C_n H_{2n+2}} = \frac{\kappa_1}{\kappa_p + \kappa_{t,p}^{(1)}} \prod_{i=2}^n \alpha_i \quad n \geq 3 \quad (S1.8)$$

64
$$R_{C_2H_4} = \kappa_{1o}^{(2)} \exp(-2c) \frac{\kappa_1}{\kappa_p + \kappa_{t,p}^{(1)}} \alpha_2 \quad (S1.9)$$

65
$$R_{1-C_n H_{2n}} = \kappa_{1o}^{(2)} \exp(-c * n) \frac{\kappa_1}{\kappa_p + \kappa_{t,p}^{(1)}} \prod_{i=2}^n \alpha_i \quad n \geq 3 \quad (S1.10)$$

$$R_{2-C_nH_{2n}} = \kappa_{t,2o}^{(2)} \frac{\kappa_1}{\kappa_p + \kappa_{t,p}^{(1)}} \prod_{i=2}^n \alpha_i \quad n \geq 4 \quad (S1.11)$$

Where, c is the carbon number correction term of the vapor-liquid equilibrium(VLE) constant of olefin, which is obtained by the modified Peng–Robinson equation of state in this study.

$$\kappa_1 = k_1 \theta_{CH_2-S} \theta_{H-S}, \quad \kappa_p = \frac{k_1 \theta_{CH_2-S}}{k_{t,p} \theta_{H-S}} \quad (S1.12)$$

$$\kappa_{t,p}^{(1)} = \frac{k_{t,p}^{(1)}}{k_{t,p}}, \quad \kappa_{t,p}^{(2)} = \frac{k_{t,p}^{(2)}}{k_{t,p}}, \quad \kappa_{t,2o} = \frac{k_{t,2o} \theta_S}{k_{t,p} \theta_{H-S}} \quad (S1.13)$$

$$K_{1o}^{(2)} = \frac{k_{t,p}^{(2)}}{(k_{t,p})^2} \frac{k_{t,1o} aSV}{k_{r,1o}^{(2)} (\theta_{H-S})^2 R_g T}, \quad K_{1o} = \frac{1}{k_{t,p}} \frac{k_{t,1o} aSV}{k_{r,1o}^{(2)} (\theta_{H-S})^2 R_g T} \quad (S1.14)$$

$$\alpha_2 = \frac{\kappa_p}{\kappa_p + k_{t,p}^{(2)} + K_{1o}^{(2)} \exp(-2c)} \quad (S1.15)$$

$$\alpha_3 = \frac{\kappa_p}{1 + \kappa_p + K_{1o} \exp(-3c)} \quad (S1.16)$$

$$\alpha_n = \frac{\kappa_p}{1 + \kappa_p + \kappa_{t,2o} + K_{1o} \exp(-cn)} \quad n \geq 4 \quad (S1.17)$$

S1.4 Single-mechanism with physisorption correction in Fig. 1b4

The study in Fig. 1b4 is carried out in slurry reactor and rate equations were based on the elementary reactions corresponding to a form of well-known carbide mechanism [5], as shown in Table S1-2.

81

82

83

84

Table S1-2 FTS reaction pathway and rate equation

Number	Step	rate equation
1 ^{RDS} -1	$CO + H-s \rightarrow H-s-CO$	$k_1 P_{CO} [H-s]$
1 ^{RDS} -2	$CO + CH_3-s \rightarrow CH_3-s-CO$	$k_1 P_{CO} [CH_3-s]$
1 ^{RDS} -n	$CO + C_n H_{2n+1}-s \rightarrow C_n H_{2n+1}-s-CO$	$k_1 P_{CO} [C_n H_{2n+1}-s]$
2-1	$H-s-CO + 2H \rightarrow H-s-C + H_2O$	K_2
2-2	$CH_3-s-CO + 2H \rightarrow CH_3-s-C + H_2O$	K_2
2-n	$C_n H_{2n+1}-s-CO + 2H \rightarrow C_n H_{2n+1}-s-C + H_2O$	K_2
3-1	$H-s-C + 2H-s \rightarrow H-s-CH_2 + 2s$	K_3
3-2	$CH_3-s-C + 2H-s \rightarrow CH_3-s-CH_2 + 2s$	K_3
	$C_n H_{2n+1}-s-C + 2H-s \rightarrow C_n H_{2n+1}-s-CH_2 + 2s$	
3-n		K_3
4	$C_n H_{2n+1}-s-CH_2 \rightarrow C_n H_{2n+1}-CH_2-s$	K_4
5 ^{RDS} -1	$CH_3-s + H_2 \rightarrow CH_4 + H-s$	$k_{5M} P_{H_2} [CH_3-s]$
5 ^{RDS} -n	$C_n H_{2n+1}-s + H_2 \rightarrow C_n H_{2n+2} + H-s$	$k_5 P_{H_2} [C_n H_{2n+1}-s]$
6 ^{RDS} -2	$CH_3CH_2-s \rightarrow C_2H_4 + H-s$	$k_{6E,0} e^{c_2} P_{H_2} [CH_3CH_2-s]$
6 ^{RDS} -n	$C_n H_{2n+1}-s \rightarrow C_n H_{2n} + H-s$	$k_{6,0} e^{c_n} P_{H_2} [C_n H_{2n+1}-s]$
7	$H_2 + 2s \leftrightarrow 2H-s$	K_7

86 In the mechanism, chain growth (step 1) and chain termination (steps 5&6) are rate-
 87 determining steps(RDS), and the rest are fast equilibrium processes. The 1-olefin
 88 desorption rate constant was assumed to be a function of carbon number due to the
 89 effect of weak interaction of the hydrocarbon chain with the catalyst surface.

90 Reaction equations of methane, ethylene, n-paraffin and 1-olefin can be written as:

$$91 \quad R_{CH_4} = k_{5M} k_7^{0.5} P_{H_2}^{1.5} \alpha_1 [S] \quad (S1.18)$$

$$92 \quad R_{C_2H_4} = k_{6E,0} e^{2c} \sqrt{K_7 P_{H_2}} \alpha_1 \alpha_2 [S] \quad (S1.19)$$

$$93 \quad R_{C_n H_{2n+2}} = k_5 k_7^{0.5} P_{H_2}^{1.5} \alpha_1 \alpha_2 \prod_{i=3}^n \alpha_i [S] \quad (S1.20)$$

$$94 \quad R_{C_n H_{2n}} = k_{6,0} e^{cn} \sqrt{K_7 P_{H_2}} \alpha_1 \alpha_2 \prod_{i=3}^n \alpha_i [S] \quad (S1.21)$$

95 Where, α is the chain growth probability factor for a molecule with n carbon atoms,

$$96 \quad \alpha_n = \frac{k_1 P_{CO}}{k_1 P_{CO} + k_5 P_{H_2} + k_{6,0} e^{cn}} \quad n \geq 3 \quad (S1.22)$$

97 Because methane and ethylene have different termination rate constants, growth
 98 probabilities for $n = 1$ and $n = 2$ should be defined separately:

$$99 \quad \alpha_1 = \frac{k_1 P_{CO}}{k_1 P_{CO} + k_{5M} P_{H_2}} \quad (S1.23)$$

$$100 \quad \alpha_2 = \frac{k_1 P_{CO}}{k_1 P_{CO} + k_5 P_{H_2} + k_{6E,0} e^{2c}} \quad (S1.24)$$

101 $[S]$ is the concentration of vacant sites,

$$102 \quad [S] = 1 / \left\{ 1 + \sqrt{K_7 P_{H_2}} + \sqrt{K_7 P_{H_2}} \left(1 + \frac{1}{K_4} + \frac{1}{K_3 K_4 P_{H_2}} + \frac{P_{H_2O}}{K_2 K_3 K_4 P_{H_2}} \right) (\alpha_1 + \alpha_1 \alpha_2 + \alpha_1 \alpha_2 \sum_{i=3}^n \prod_{j=3}^i \alpha_j) \right\} \quad (S1.25)$$

103 c is the carbon number correction for the olefin desorption constant,

$$104 \quad c = -\frac{\Delta E}{RT} \quad (S1.26)$$

105 Where, ΔE is a contribution in the increase of desorption energy per every $-CH_2-$
 106 group.

107

108 **S1.5 Single-mechanism in Fig. 1b5**

109 This study was carried out in a fixed bed micro-reactor, and on the basis of proposed
 110 reaction mechanisms, developed according to the carbide theory and the alkyl
 111 mechanism, the kinetic expressions for n-paraffins and α -olefins formation are derived
 112 [6]. The elementary reaction and rate equation are shown in Table S1-3.

113

114

115

116

117

118

Table S1-3 Mechanism of carbide in FTS

Number	Step	rate equation
1	$H_2 + 2s \rightarrow 2H - s$	$r_{H_2} = k_{H_2} P_{H_2} \theta^2 \theta_{H^*}^{-1}$
2a	$CO + s \rightarrow CO - s$	$r_M = k_M P_{CO} \theta$
2b	$CO - s + s \rightarrow C - s + O - s$	--
2c	$C - s + H - s \rightarrow CH - s + s$	--
2d	$CH - s + H - s \rightarrow CH_2 - s + s$	--
2e	$O - s + H - s \rightarrow OH - s + s$	--
2f	$OH - s + H - s \rightarrow H_2O + 2s$	--
3	$CH_2 - s + H - s \rightarrow CH_3 - s + s$	$r_{IN} = k_{IN} \theta_{CH_2-s} \theta_{H-s}$
4	$CH_3 - s + H - s \rightarrow CH_4 + 2s$	$r_{CH_4} = k_{CH_4} \theta_{CH_3-s} \theta_{H-s}$
5	$C_n H_{2n+1} - s + CH_2 - s \rightarrow C_{n+1} H_{2n+3} - s + s$	$r_{G,n} = k_G \cdot \theta_{C_n H_{2n+1}-s} \theta_{CH_2-s}$
6	$C_n H_{2n+1} - s + H - s \rightarrow C_n H_{2n+2} + 2s$	$r_{P,n} = k_{Pn} \cdot \theta_{C_n H_{2n+1}-s} \theta_{H-s}$
7	$C_n H_{2n+1} - s \leftrightarrow C_n H_{2n} + H - s$	$r_{O,n} = k_{O_n,dx} \theta_{C_n H_{2n+1}-s} - k_{O_n,sx} x_{C_n H_{2n}} \theta_{H-s}$
8	$C_2 H_5 - s \leftrightarrow C_2 H_4 + H - s$	$r_{O,2} = k_{O_2,dx} \theta_{C_2 H_5-s} - k_{O_2,sx} x_{C_2 H_4} \theta_{H-s}$

119 Where P_n and O_n are the linear paraffin and α -olefin with n carbon atoms,
 120 respectively, θ is the fraction of free catalytic sites and x_{O_n} is the molar fraction of the
 121 α -olefin with n carbon atoms in the liquid phase surrounding the catalyst pellets.

122 In the given mechanism, H_2 is irreversibly split at the active site (s), and only the rate
 123 equation for this reaction is expressed in the model using a power law expression. CO
 124 is first adsorbed at the active site and then directly dissociated, assuming that step (2a)
 125 is a rate-determining in the sequence of consecutive non-reversible steps (2a~f). The
 126 rate constants for chain growth (step 5) and chain termination (step 6 and step 7) are
 127 independent of the carbon number. To describe the experimental deviations of methane
 128 and ethylene, the rate constants in step 4 and step 8 were treated separately.

129 S1.6 Dual-mechanism in Fig. 1b6

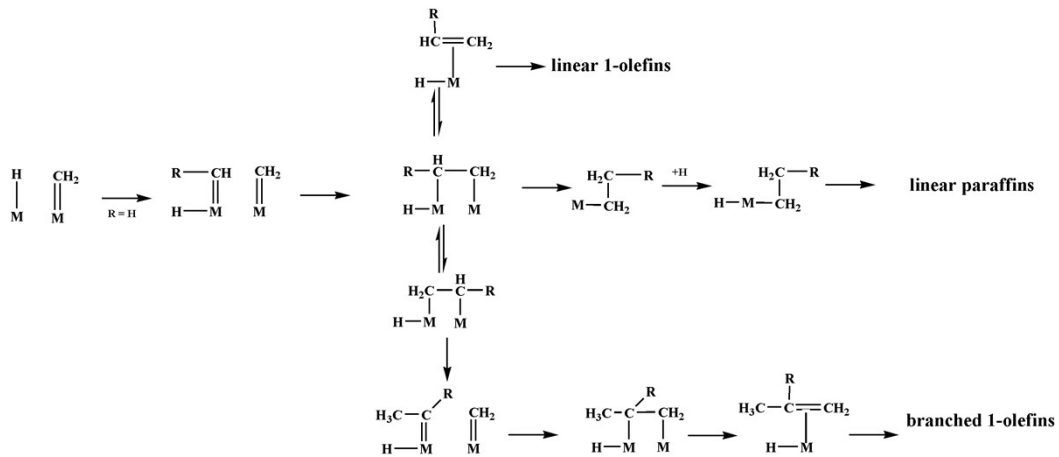
130 This model is proposed based on the hypothesis that two incompatible mechanisms
 131 are involved resting exclusively on methylene (Fig. S1-2) and on carbon monoxide

132 insertion(Fig. S1-3), respectively. Each mechanism individually conforms to the linear
 133 relationship of the Schulz-Flory model, and the product distribution in the experiment
 134 is a superposition of the two mechanisms [7].

135 In the dual-mechanism model, the molar fraction (x_i) of the product is expressed as

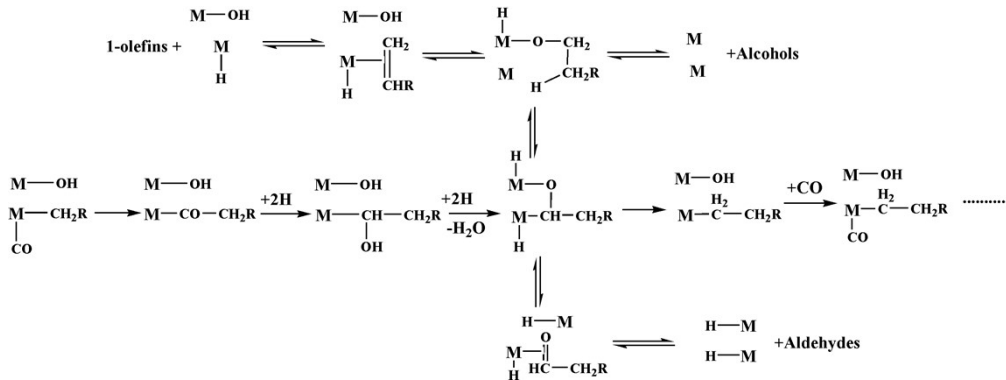
$$136 \quad \frac{x_i}{1 - x_1^{\text{exp}} - x_2^{\text{exp}}} = \frac{\alpha_1^{i-1} + \left(\frac{\alpha_1}{\alpha_2}\right)^{\xi-1} \alpha_2^{i-1}}{\frac{\alpha_1^2}{1 - \alpha_1} + \left(\frac{\alpha_1}{\alpha_2}\right)^{\xi-1} \frac{\alpha_2^2}{1 - \alpha_2}} \quad (\text{S1.27})$$

137 Where, x_1^{exp} and x_2^{exp} are the molar fractions of methane and ethylene. α_1 and α_2 are
 138 chain growth probability factors, ξ is the intersection point of the two product
 139 distributions, and these three parameters are evaluated by the least squares method.



140

141 **Fig. S1-2 Mechanism 1: monomer CH₂**



142

143 **Fig. S1-3 Mechanism 2: monomer CO**

144

145

146 **S1.7 Dual-mechanism in Fig. 1b7**

147 Fig. 1b7 uses vapour–liquid equilibrium (VLE) to explain the observed dual- α
148 product distribution in FTS. In their model, a single distribution is set up in the liquid
149 phase, and the vapour is in equilibrium with the liquid [8].

150 The molar fraction of hydrocarbons with carbon number n in the gas phase (y_n) and
151 liquid phase (x_n) can be expressed as,

152
$$x_n = \alpha^{n-1}(1-\alpha)(1-c) \quad (\text{S1.28})$$

153
$$y_n = K_n \alpha^{n-1}(1-\alpha)(1-c) \quad (\text{S1.29})$$

154 Where, α is the chain growth factor, which is a constant independent of carbon
155 number. K_n is the VLE constant, and c is the total molar fraction of the components in
156 the liquid phase other than hydrocarbons. the total product distribution is described by

157
$$\frac{z_{n+1}}{z_n} = \frac{x_{n+1}}{x_n} \frac{fK_{n+1} + (1-f)}{fK_{n+1} + (1-f)} = \alpha \frac{fK_{n+1} + (1-f)}{fK_n + (1-f)} \quad (\text{S1.30})$$

158 z_n is the total mole fraction of hydrocarbon with carbon number n . f is the fraction of
159 gas phase, $f = \frac{V}{Z}$.

160 For lighter hydrocarbons (small n), $K_n \gg 1$,

161
$$\frac{z_{n+1}}{z_n} = \alpha \frac{K_{n+1}}{K_n} = \alpha\beta \quad (\text{S1.31})$$

162 For heavier hydrocarbons (large n), $K_n = 1$,

163
$$\frac{z_{n+1}}{z_n} = \alpha \quad (\text{S1.32})$$

164 Thus the total product distribution for lighter hydrocarbons follows the vapour phase
165 distribution where the slope is given by $\log(\alpha\beta)$. On the other hand, the total product

166 distribution for heavier hydrocarbons is consistent with the liquid phase product
 167 distribution where the slope is given by $\log(\alpha)$. This clearly shows the observed
 168 deviation from the single alpha Schulz-Flory distribution.

169 **S1.8 Multi-site in Fig. 1b8**

170 Fig 1b8 includes two-site model and distributed-site model. In two-site model the
 171 molecular weight distribution of the products is described with a modification of the
 172 Schulz-Flory distribution by including a second site, as shown in Eq. S1.33.

$$173 \quad m_n = x(1 - \alpha_1)\alpha_1^{n-1} + (1 - x)(1 - \alpha_2)\alpha_2^{n-1} \quad (S1.33)$$

174 Where m_n is the total moles of carbon number n relative to the total moles of organic
 175 product, α_1 and α_2 are the chain growth probabilities for two active-sites, and x is the
 176 mole fraction of organic product synthesized on site 1.

177 In the multi-site model, the molar fraction of substance with carbon number n is,

$$178 \quad m_n = \frac{\int_0^\infty F(X)(1 - \alpha(X))\alpha(X)^{n-1} dx}{\sum_{n=1}^\infty \int_0^\infty F(X)(1 - \alpha(X))\alpha(X)^{n-1} dx} \quad (S1.34)$$

179 This model introduces a dimensionless random variable X based on the Schulz-Flory
 180 model and assumes that it is proportional to the concentration of potassium relative to
 181 iron at a given point on the catalyst surface^[9]. Postulating that potassium is normally
 182 distributed on the catalyst surface, the fraction of sites with a potassium concentration
 183 X , is given by,

$$184 \quad F(X) = \frac{1}{\sqrt{2\pi}} \exp(X - X_{sm})^2 \quad (S1.35)$$

185 where X_{sm} is the potassium concentration of maximum probability.

186 The chain growth factor can be expressed as a function of X ,

187

$$\alpha(X) = 1 - (1 - \alpha_0) \exp(-bX) \quad (\text{S1.36})$$

188

where α_0 is the chain growth probability at $X = 0$ (pure iron). The parameter b

189

represents the strength of interaction between neighboring potassium and iron atoms.

190

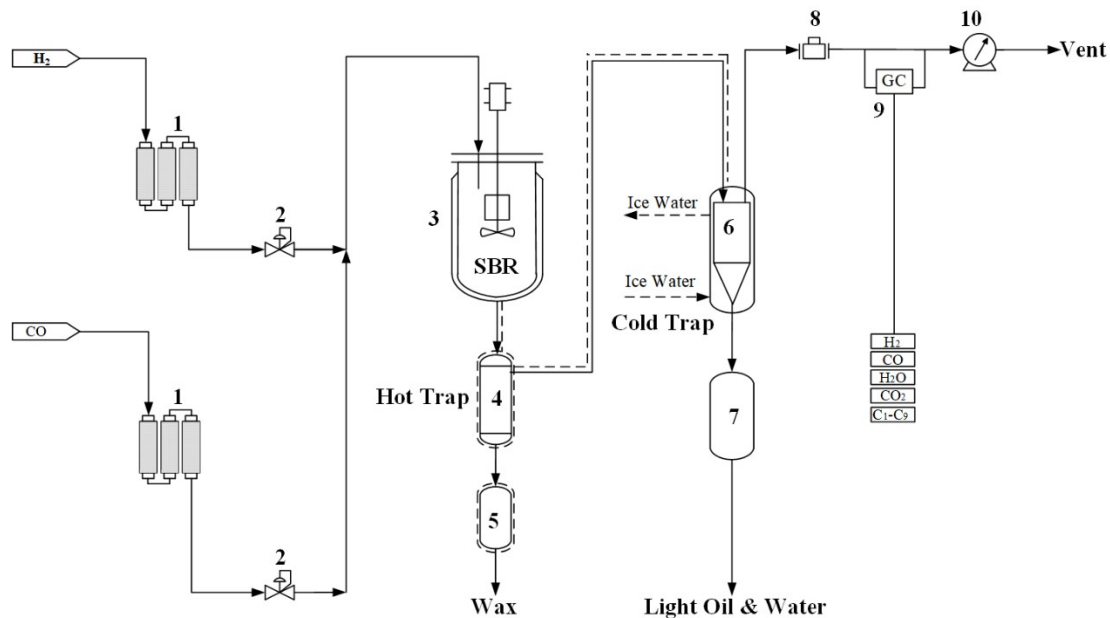
As b approaches zero, α approaches α_0 since at this limit the iron acts independently of

191

the potassium.

192

193 S2 The detailed flow diagrams of the reactors



194

195

Fig. S2-1 Flow scheme of the Spinning Basket Reactor

196

1. purification unit (de-sulphur, de-oxygen, de-carbonyl, de-water); 2. mass flow controller (Both

197

H₂ and CO); 3. Spinning Basket Reactor (SBR), 4. Hot trap; 5. Buff tank1(for wax); 6. Cold trap;

198

7. Buff tank2 (for light oil and water); 8. back pressure regulator; 9. Gas Chromatography (GC, for

199

tailgas); 10.wet flow meter.

200

The experimental process with SBR is shown in Fig. S2-1. After purification

201

(desulfurization, dehydration, decarbonylation), H₂ and CO are mixed at set flow rates

202

by mass flow controller, enter into the SBR and contact with the catalysts to undergo

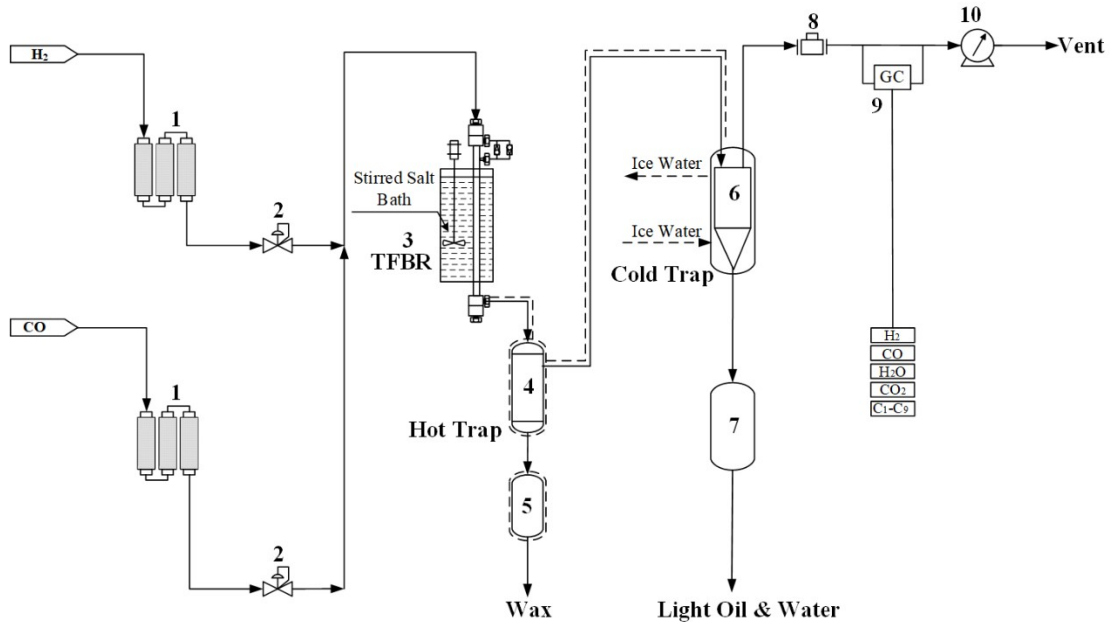
203

FTS. The gas-liquid mixture of the reactor effluent is firstly separated by a hot trap to

204

obtain wax. The rest enters into a cold trap and cools to obtain the light oil and water.

205 After decompression, the non-condensable gas is analyzed online and then enters the
 206 wet flow meter for flow measurement.



207

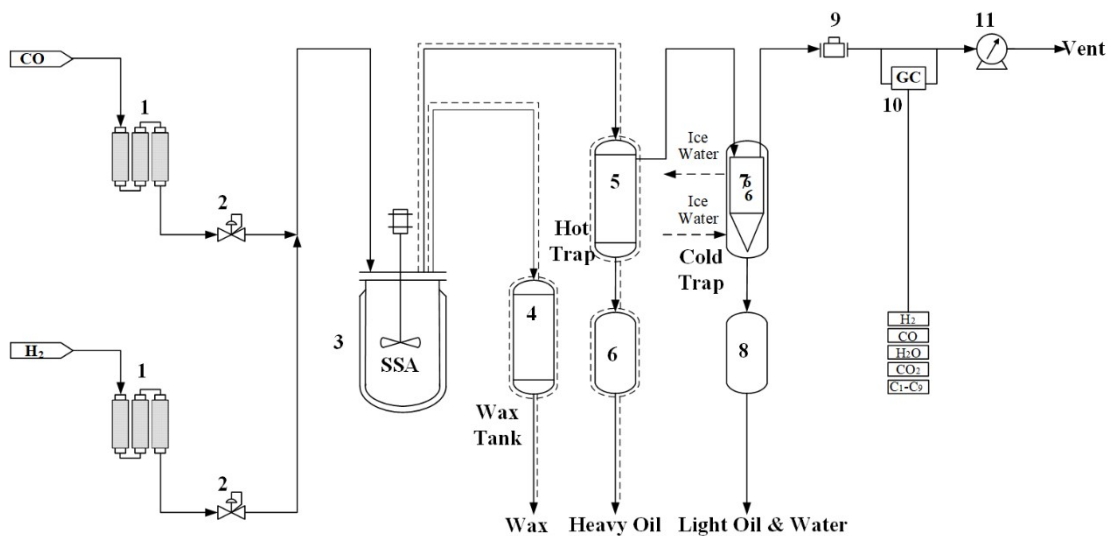
208

Fig. S2-2 Flow scheme of the Tubular Fixed-Bed Reactor

209 1. purification unit (de-sulphur, de-oxygen, de-carbonyl, de-water); 2. mass flow controller (Both
 210 H₂ and CO); 3. Tubular Fixed-Bed Reactor (TFBR), 4. Hot trap; 5. Buff tank1 (for wax); 6. Cold
 211 trap; 7. Buff tank2 (for light oil and water); 8. back pressure regulator, 9. Gas Chromatography
 212 (GC, for tail gas); 10. wet flow meter.

213 The flow scheme of the Tubular Fixed-Bed Reactor (TFBR) is similar to that of the

214 SBR, except for the reactor itself (Fig. S2-2).



215

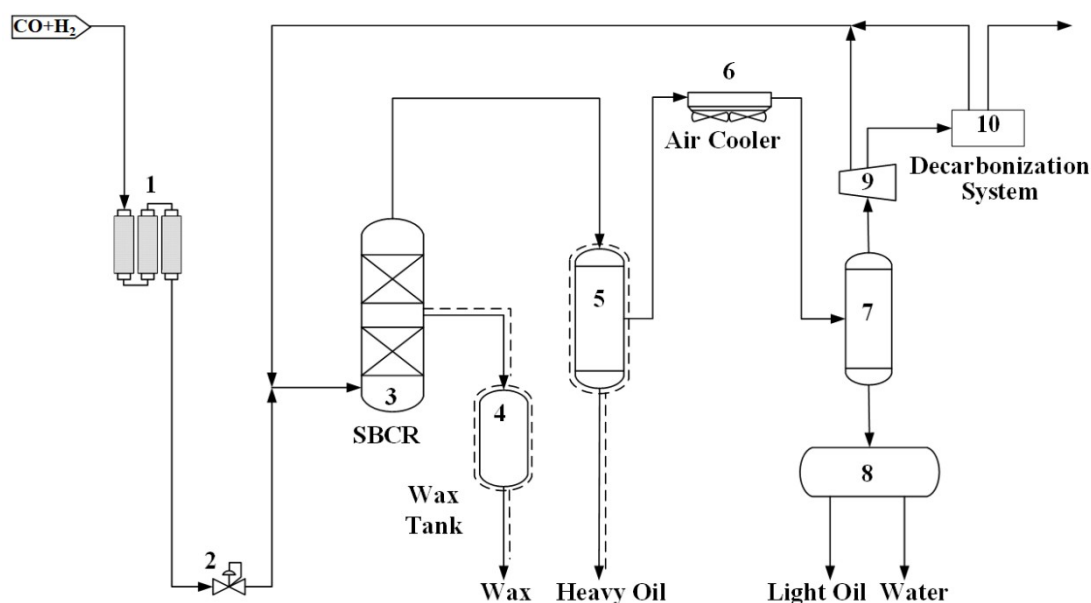
216

Fig. S2-3 Flow scheme of the Stirred Slurry Autoclave

217 1. purification unit (de-sulphur, de-oxygen, de-carbonyl, de-water); 2. mass flow controller (Both
 218 H₂ and CO); 3. Stirred Slurry Autoclave (SSA); 4. Wax Tank; 5. Hot trap; 6. Buff tank1 (for
 219 heavy oil); 7. Cold trap; 8. Buff tank2 (for light oil and water); 9. back pressure regulator, 10. Gas
 220 Chromatography (GC, for tailgas); 11. wet flow meter.

221 The product collection process in Stirred Slurry Autoclave (SSA) is different from
 222 the above process in some extent (Fig. S2-3), e.g., the wax is collected through a Wax
 223 Tank, and the remaining components enter into a hot trap to collect the heavy oil, and
 224 then the rests enter into a cold trap to cool down and get light oil and water. After
 225 decompression the non-condensable gas is analyzed online and then enters into a wet
 226 flow meter for quantity measurement. Here, the heavy oil and light oils are normally
 227 mixed together for analysis.

228



229

230 **Fig. S2-4** Flow scheme of the industrial Slurry Bubble Column Reactor

231 1. purification unit (de-sulphur, de-oxygen, de-carbonyl, de-water); 2. mass flow controller; 3.
 232 Slurry Bubble Column Reactor (SBCR); 4. Wax Tank; 5. Gas-liquid separator1 (for heavy oil); 6.
 233 Air Cooler; 7. Gas-liquid separator2 (for light oil and water); 8. Oil-water separator; 9.
 234 Compressor; 10. Decarbonization system.

235 The process flow and product collection in the Slurry Bubble Column Reactor
 236 (SBCR) are similar to that of the SSA process, as shown in Fig. S2-4. The purified
 237 syngas(H₂+CO) is injected into the SBCR, where it undergoes FTS upon contacting

238 with the catalyst. The produced liquid wax is collected in a wax tank, while the gas
239 phase products at the top of the SBCR proceeds to gas-liquid separator 1 to obtain heavy
240 oil. The remaining gas is cooled and then directed to gas-liquid separator 2, where light
241 oil and water are obtained. Upon compression, the non-condensable gas enters the
242 decarbonization system. After removing most of the CO₂, a portion returns to the
243 reactor, while the remainder enters the subsequent unit.

244

245 **S3 The detailed experimental process for data collection**

246 **Data collection in the Slurry Bubble Column Reactor (SBCR):** The SBCR is an
247 industrial reactor located at Yitai Hangjinqi plant in China. Under normal
248 circumstances, the reactor maintains long-term stable industrial operating conditions.
249 The running results under this condition has undergone extensive duplicate validations.
250 We collected 24-hour products for material balance checking, product analysis and data
251 processing.

252 **Data collection in the Stirred Slurry Autoclave (SSA):** Experiments in SSA
253 required additional liquid paraffins as an initial solvent for catalyst dispersion. After
254 catalyst reduction and approximately 8 days of solvent replacement at the reaction
255 conditions, no visually discernible solvent peaks were detected in collected oil and was
256 samples. Subsequently, we maintained the reaction conditions for 24 hours and
257 continuously analyzed the tail gas for steady-state confirmation, and then collected 12-
258 hour products several times for material balance checking, product analysis and data
259 processing.

260 **Data collection in the Tubular Fixed-Bed Reactor (TFBR):** The TFBR requires
261 careful catalyst dilution and loading to ensure consistent repeatability across multiple
262 experiments. After catalyst reduction and stability evaluation under the reaction
263 conditions (by monitoring the repeatability of the tail gas composition) for 72 hours,
264 then collected 12-hour products several times for material balance checking, product
265 analysis and data processing.

266 **Data collection in the Spinning Basket Reactor (SBR):** The distribution behavior
267 of FTS product under various reaction conditions was extensively investigated in the
268 SBR reactor. When switching to a new experimental point, we maintained the reaction
269 conditions for 24 hours and continuously analyzed the tail gas for steady-state
270 confirmation, and then collected 12-hour products two times for material balance
271 checking, product analysis and data processing. A standard point (275 °C, 3.0 MPa,
272 $H_2/CO = 3$, GHSV=3.5 NL/h/g-cat) was set to check whether the catalyst has undergone
273 deactivation and requires replacement with a new catalyst. The standard point was
274 repeated every 5 experimental points to do the evaluation.
275

276 **S4 The detailed calculation methodology for determining the overall** 277 **product distribution**

278 The Fischer-Tropsch synthesis products exhibit a broad boiling range, necessitating
279 multi-stage cooling for their separation and collection. The effluent streams consist of
280 the tail gas, oil, wax and aqueous products. The total mass of the hydrocarbon and
281 oxygenate products is defined

282
$$M_{total} = M_{gas} + M_{oil} + M_{wax} + M_{aqueous} \quad (S4.1)$$

283 in which M_{gas} is the mass of the hydrocarbon products in the tail gas stream, $M_{aqueous}$ is
 284 the mass of the oxygenates in the aqueous phase.

285 The mass of each component in a stream is defined by $M_{n,stream}^i$, where *stream*
 286 represents tail gas, oil, wax or aqueous stream, *i* is the type of a component, e.g., olefin,
 287 paraffin, alcohol, acid, aldehyde, ketone and ester, *n* is the carbon number of the
 288 component.

289 The mass of a component in the tail gas is quantified by 1D GC

290
$$M_{n,gas}^i = \frac{f_{n,gas,1D}^i * A_{n,gas,1D}^i}{\sum f_{n,gas,1D}^i * A_{n,gas,1D}^i} \frac{V_{gas}}{22.4} * m_n^i \quad (S4.2)$$

291 where, $f_{n,gas,1D}^i$ and $A_{n,gas,1D}^i$ are the molar response factor and peak area of a gas
 292 component with type *i* and carbon number *n* characterized in 1D GC, respectively.
 293 V_{gas} is the volume flow rate of the tail gas at standard conditions, m_n^i is the molecular
 294 weight of the component with type *i* and carbon number *n*.

295 The oil is analyzed by both 1D GC and 2D GC×GC. The 1D GC is responsible for
 296 quantifying components with carbon number ≤ 7 , while the 2D GC×GC quantifying
 297 the rest parts. The 1D GC and 2D GC×GC results are correlated by using C10 paraffin
 298 as an internal standard

299
$$f_{n,oil,2D}^i * A_{n,oil,2D}^i = \frac{f_{10,2D}^{paraffin} * A_{10,2D}^{paraffin}}{f_{10,1D}^{paraffin} * A_{10,1D}^{paraffin}} * f_{n,oil,1D}^i * A_{n,oil,1D}^i \quad n \leq 7 \quad (S4.3)$$

300 where $f_{n,oil,1D}^i$ and $f_{n,oil,2D}^i$ are the mass response factors of an oil component with type
 301 *i* and carbon number *n* characterized in 1D GC and 2D GC×GC, respectively.

302 $A_{n,oil,1D}^i$ and $A_{n,oil,2D}^i$ are the peak areas of the corresponding component in 1D GC and

303 2D GC×GC, respectively. C10 paraffin is the internal standard. Therefore, the mass
 304 of a component in the oil could be calculated

$$305 \quad M_{n,oil}^i = \frac{f_{n,oil,2D}^i * A_{n,oil,2D}^i}{\sum f_{n,oil,2D}^i * A_{n,oil,2D}^i} M_{oil} \quad (S4.4)$$

306 The components with carbon number ≤ 30 in wax are quantified by 2D GC×GC,

$$307 \quad M_{n,wax}^i = \frac{f_{n,wax,2D}^i * A_{n,wax,2D}^i}{\sum f_{n,wax,2D}^i * A_{n,wax,2D}^i} M_{wax} * RM_{30} \quad n \leq 30 \quad (S4.5)$$

308 where $f_{n,wax,2D}^i$ and $A_{n,wax,2D}^i$ are the mass response factor and peak area of a wax
 309 component with type i and carbon number n characterized in 2D GC×GC, respectively.

310 RM_{30} is the recovered mass% of wax components at C30.

311 The components with carbon number > 30 in wax are quantified by high temperature
 312 simulated distillation (HTSD) which could provide the mass information of each carbon
 313 number.

$$314 \quad M_{n,wax} = \frac{f_{n,wax,HTSD} * A_{n,wax,HTSD}}{\sum f_{n,wax,HTSD} * A_{n,wax,HTSD}} M_{wax} * (RM_{100} - RM_{30}) \quad 30 < n \leq 100 \quad (S4.6)$$

315 where $f_{n,wax,HTSD}$ and $A_{n,wax,HTSD}$ are the mass response factors and peak area of a wax
 316 component with carbon number n characterized in HTSD, respectively. RM_{100} is the
 317 recovered mass% of wax components at C100.

318 Subsequently, the mass fractions of paraffins and olefins with carbon number ≤ 30
 319 and the mass fractions of the total hydrocarbons with carbon number ≤ 100 can be
 320 calculated, thereby obtaining the related product distribution curve

$$321 \quad W_n^{paraffin} = \frac{M_{n,gas}^{paraffin} + M_{n,oil}^{paraffin} + M_{n,wax}^{paraffin}}{M_{total}} \quad 1 \leq n \leq 30 \quad (S4.7)$$

$$322 \quad W_n^{olefin} = \frac{M_{n,gas}^{olefin} + M_{n,oil}^{olefin} + M_{n,wax}^{olefin}}{M_{total}} \quad 2 \leq n \leq 30 \quad (S4.8)$$

323
$$W_n = W_n^{olefin} + W_n^{paraffin} \quad 1 \leq n \leq 30 \quad (S4.9)$$

324
$$W_n = \frac{M_{n,wax}}{M_{total}} \quad 30 < n \leq 100 \quad (S4.10)$$

325 where $W_n^{paraffin}$, W_n^{olefin} and W_n are mass fractions of a paraffin, olefin and total
 326 hydrocarbon with carbon number n .

327 HTSD can only provide the mass of each carbon number, but our previous results
 328 show that C30+ wax consists almost entirely of paraffins, with very few amounts of
 329 olefins, and the oxygenates are negligible. To be accurate, we can estimate the olefin
 330 distribution in C30+ wax by extrapolating the known distribution of C15-C30 olefin,
 331 then obtain the paraffin distribution with carbon number $30 < n \leq 100$ by subtracting
 332 the olefin distribution from the carbon number distribution

333
$$W_n^{olefin} = n e^{b_o} (\alpha_o)^n \quad 30 < n \leq 100 \quad (S4.11)$$

334
$$W_n^{paraffin} = W_n - W_n^{olefin} \quad 30 < n \leq 100 \quad (S4.12)$$

335 where α_o and b_o could be estimated from the known carbon number distribution of
 336 olefin.

337 According to extensive experimental data, we observed that the chain growth factor
 338 at the high-carbon-number range remained approximately invariant with carbon
 339 number. Therefore, the unrecovered section of wax could reasonably be complemented
 340 by extrapolating the known total hydrocarbon distribution curve

341
$$W_n = n e^b \alpha^n \quad 100 < n \leq N \quad (S4.13)$$

342 where α and b could be estimated from the known total hydrocarbon distribution. N is
 343 the maximum carbon number to be extrapolated and it is determined by the following
 344 constraints

345
$$1 - \frac{RM_{100}}{100} - \sum_{n=101}^N \frac{W_n M_{total}}{M_{wax}} \leq 0.001 \quad (S4.14)$$

346 which means the content of each carbon number in the unrecovered wax is extrapolated
 347 according to equation (S4.13) until the extrapolation reaches a carbon number N where
 348 the unrecovered mass is less than 0.1%.

349 The above constraints originate from the following two equations

350
$$W_{n,wax} = W_n \frac{M_{total}}{M_{wax}} \quad 100 < n \leq N \quad (S4.15)$$

351
$$1 - \frac{RM_{100}}{100} = \sum_{n=101}^N W_{n,wax} = \sum_{n=101}^N \frac{W_n M_{total}}{M_{wax}} \quad (S4.16)$$

352 **S5 Operating conditions and results**

353 The operating conditions and results mentioned in Fig. 2 to Fig. 4 are shown in Table S5-1.

354 **Table S5-1** Reaction conditions and experimental results

No	T K	P Mpa	inlet H ₂ /CO --	inlet GHSV NL/g-cat/h	outlet GHSV NL/g-cat/h	xCO %	xH ₂ %	Selectivity(C-atom%)		
								CH ₄	C ₂ ~C ₄	C ₅ +
R-1	273	2.92	2.88	19.40	--	63.83	25	2.55	4.31	74.21
R-2	275	3.01	3.00	10.00	7.49	74.67	28.79	4.33	10.34	56.42
R-3	275	3.00	3.01	10.00	7.74	61.4	25.8	3.09	9.91	58.56
R-4*	275	3.00	2.99	10.01	7.64	64.7	27.26	6.94	8.91	46.22
HC-1	275	3.01	1.00	35.01	29.43	25.41	25.49	1.14	5.33	57.14
HC-2	275	3.03	2.00	35.00	29.61	35.43	19.23	1.97	6.77	58.03
HC-4	275	3.03	4.00	34.99	30.63	49.11	14.16	3.44	6.75	65.25
HC-5	275	3.03	5.00	34.99	30.48	58.88	13.81	4.49	7.19	60.62
SV-10*	275	3.00	2.99	10.01	7.64	64.7	27.26	6.94	8.91	46.22
SV-25	275	3.00	3.00	25.00	21.22	44.42	17.36	6.16	10.32	49.39
SV-60	275	3.03	3.00	60.00	54.19	32.24	11.17	4.1	13.33	54.37
T-265	265	3.00	3.00	35.00	28.99	44.69	20.56	2.06	6.81	63.79
T-275	275	3.03	3.00	35.00	29.49	47.78	18.09	2.34	6.08	63.12
T-285	285	3.00	3.00	35.00	28.73	50.65	22.02	2.76	6.52	67.72
T-295	295	3.00	3.00	35.00	28.83	53.27	21.08	3.18	6.76	61.31

355 Note: R-4 and SV-10 are the same experimental point.

356

357 The original experimental data in the manuscript are shown in Table S5-2~S5-5, including total hydrocarbons, olefins and paraffins and their
 358 extrapolations.

359 **Table S5-2** The detailed data of the total hydrocarbon distribution in Fig. 2c, Fig. 4a1-Fig. 4d1

C	R1	R2	R3	R4	HC-1	HC-2	HC-4	HC-5	SV-10	SV-25	SV-60	T-265	T-275	T-285	T-295
1	-3.234	-2.745	-3.073	-2.168	-3.926	-3.439	-3.003	-2.696	-2.168	-2.337	-2.736	-3.475	-3.331	-3.266	-3.030
2	-5.014	-4.084	-4.307	-3.841	-4.561	-4.396	-4.764	-4.695	-3.841	-3.758	-4.071	-4.516	-4.692	-4.873	-4.690
3	-4.635	-3.966	-4.086	-4.119	-4.534	-4.331	-4.507	-4.400	-4.119	-3.987	-4.083	-4.407	-4.518	-4.581	-4.455
4	-4.934	-4.371	-4.267	-4.490	-4.936	-4.748	-4.644	-4.510	-4.490	-4.468	-4.511	-4.786	-4.786	-4.704	-4.581
5	-5.202	-4.760	-4.484	-4.722	-5.293	-5.128	-4.817	-4.675	-4.722	-4.788	-4.869	-5.154	-5.054	-4.871	-4.754
6	-5.280	-5.067	-4.699	-4.941	-5.598	-5.383	-5.044	-4.883	-4.941	-5.007	-5.183	-5.494	-5.253	-5.049	-4.940
7	-5.297	-5.298	-4.901	-5.112	-5.962	-5.758	-5.219	-5.042	-5.112	-5.167	-5.431	-5.763	-5.385	-5.172	-5.091
8	-5.388	-5.505	-5.077	-5.281	-6.128	-5.901	-5.350	-5.168	-5.281	-5.316	-5.597	-5.911	-5.505	-5.285	-5.217
9	-5.516	-5.683	-5.259	-5.438	-6.286	-6.062	-5.498	-5.326	-5.438	-5.479	-5.758	-6.060	-5.641	-5.428	-5.377
10	-5.656	-5.851	-5.445	-5.617	-6.416	-6.190	-5.631	-5.478	-5.617	-5.645	-5.882	-6.166	-5.774	-5.563	-5.513
11	-5.816	-6.025	-5.624	-5.783	-6.559	-6.319	-5.774	-5.637	-5.783	-5.803	-6.011	-6.296	-5.905	-5.691	-5.665
12	-5.980	-6.181	-5.809	-5.941	-6.684	-6.444	-5.923	-5.800	-5.941	-5.964	-6.144	-6.399	-6.040	-5.824	-5.823
13	-6.132	-6.351	-6.008	-6.107	-6.793	-6.564	-6.072	-5.963	-6.107	-6.153	-6.273	-6.522	-6.178	-5.970	-5.993
14	-6.247	-6.473	-6.185	-6.239	-6.900	-6.669	-6.224	-6.121	-6.239	-6.325	-6.388	-6.616	-6.295	-6.096	-6.151
15	-6.355	-6.595	-6.365	-6.372	-6.984	-6.766	-6.359	-6.275	-6.372	-6.525	-6.490	-6.701	-6.406	-6.218	-6.312
16	-6.455	-6.700	-6.529	-6.499	-7.074	-6.854	-6.480	-6.400	-6.499	-6.714	-6.607	-6.780	-6.503	-6.339	-6.466
17	-6.540	-6.803	-6.677	-6.616	-7.173	-6.918	-6.585	-6.523	-6.616	-6.880	-6.711	-6.851	-6.589	-6.456	-6.605
18	-6.641	-6.900	-6.803	-6.742	-7.232	-6.982	-6.695	-6.647	-6.742	-7.025	-6.807	-6.940	-6.678	-6.579	-6.725
19	-6.762	-6.975	-6.898	-6.844	-7.288	-7.076	-6.805	-6.770	-6.844	-7.115	-6.875	-7.017	-6.736	-6.677	-6.829
20	-6.861	-7.083	-7.050	-7.018	-7.344	-7.129	-6.910	-6.930	-7.018	-7.259	-6.982	-7.048	-6.833	-6.803	-6.917

21	-6.983	-7.172	-7.140	-7.192	-7.362	-7.152	-6.994	-6.991	-7.192	-7.370	-7.069	-7.123	-6.907	-6.917	-7.005
22	-7.107	-7.261	-7.273	-7.386	-7.413	-7.222	-7.096	-7.126	-7.386	-7.465	-7.159	-7.175	-6.988	-7.029	-7.091
23	-7.220	-7.354	-7.404	-7.576	-7.458	-7.288	-7.224	-7.282	-7.576	-7.553	-7.252	-7.222	-7.072	-7.138	-7.183
24	-7.327	-7.448	-7.578	-7.746	-7.522	-7.347	-7.328	-7.373	-7.746	-7.642	-7.334	-7.275	-7.151	-7.255	-7.279
25	-7.433	-7.542	-7.693	-7.922	-7.551	-7.404	-7.442	-7.480	-7.922	-7.727	-7.420	-7.331	-7.251	-7.361	-7.377
26	-7.529	-7.637	-7.948	-8.083	-7.609	-7.511	-7.544	-7.628	-8.083	-7.837	-7.509	-7.388	-7.340	-7.469	-7.481
27	-7.624	-7.741	-8.111	-8.231	-7.663	-7.572	-7.623	-7.708	-8.231	-7.945	-7.596	-7.450	-7.427	-7.530	-7.589
28	-7.714	-7.843	-8.251	-8.369	-7.722	-7.652	-7.699	-7.805	-8.369	-8.052	-7.686	-7.517	-7.516	-7.698	-7.704
29	-7.804	-7.943	-8.381	-8.503	-7.781	-7.709	-7.790	-7.936	-8.503	-8.164	-7.776	-7.585	-7.603	-7.810	-7.817
30	-7.880	-8.042	-8.518	-8.638	-7.833	-7.780	-7.912	-8.023	-8.638	-8.277	-7.868	-7.651	-7.691	-7.915	-7.934
31	-7.982	-8.143	-8.643	-8.789	-7.857	-7.799	-8.008	-8.209	-8.789	-8.400	-7.973	-7.723	-7.783	-8.026	-8.054
32	-8.063	-8.231	-8.765	-8.924	-7.909	-7.868	-8.109	-8.322	-8.924	-8.512	-8.062	-7.787	-7.870	-8.129	-8.168
33	-8.135	-8.319	-8.894	-9.063	-7.963	-7.937	-8.208	-8.436	-9.063	-8.622	-8.150	-7.848	-7.953	-8.231	-8.282
34	-8.201	-8.409	-9.020	-9.208	-8.017	-8.006	-8.309	-8.547	-9.208	-8.732	-8.237	-7.913	-8.040	-8.332	-8.398
35	-8.259	-8.498	-9.139	-9.353	-8.073	-8.076	-8.409	-8.659	-9.353	-8.836	-8.324	-7.978	-8.124	-8.434	-8.512
36	-8.328	-8.587	-9.290	-9.498	-8.127	-8.144	-8.510	-8.774	-9.498	-8.944	-8.409	-8.043	-8.205	-8.536	-8.622
37	-8.386	-8.672	-9.345	-9.640	-8.183	-8.212	-8.608	-8.887	-9.640	-9.048	-8.495	-8.108	-8.291	-8.624	-8.737
38	-8.465	-8.763	-9.433	-9.783	-8.236	-8.281	-8.707	-8.998	-9.783	-9.153	-8.579	-8.173	-8.374	-8.724	-8.840
39	-8.525	-8.847	-9.524	-9.921	-8.289	-8.346	-8.806	-9.110	-9.921	-9.257	-8.664	-8.234	-8.458	-8.815	-8.947
40	-8.580	-8.935	-9.630	-10.059	-8.342	-8.411	-8.903	-9.218	-10.059	-9.361	-8.746	-8.296	-8.545	-8.908	-9.047
41	-8.637	-9.017	-9.765	-10.206	-8.393	-8.476	-8.997	-9.328	-10.206	-9.469	-8.829	-8.359	-8.625	-8.995	-9.148
42	-8.694	-9.102	-9.908	-10.348	-8.446	-8.537	-9.093	-9.435	-10.348	-9.574	-8.912	-8.418	-8.708	-9.086	-9.241
43	-8.773	-9.183	-10.044	-10.490	-8.501	-8.602	-9.186	-9.542	-10.490	-9.679	-8.994	-8.483	-8.792	-9.175	-9.338
44	-8.841	-9.263	-10.179	-10.632	-8.554	-8.665	-9.278	-9.647	-10.632	-9.782	-9.081	-8.546	-8.876	-9.263	-9.432
45	-8.915	-9.347	-10.304	-10.775	-8.610	-8.728	-9.372	-9.755	-10.775	-9.885	-9.170	-8.615	-8.960	-9.358	-9.527
46	-8.992	-9.429	-10.419	-10.917	-8.667	-8.793	-9.463	-9.858	-10.917	-9.984	-9.262	-8.685	-9.048	-9.449	-9.619

47	-9.053	-9.511	-10.513	-11.059	-8.727	-8.863	-9.553	-9.966	-11.059	-10.084	-9.359	-8.757	-9.135	-9.545	-9.715
48	-9.130	-9.594	-10.619	-11.201	-8.789	-8.929	-9.645	-10.071	-11.201	-10.186	-9.456	-8.832	-9.231	-9.639	-9.809
49	-9.191	-9.679	-10.733	-11.343	-8.857	-9.002	-9.738	-10.177	-11.343	-10.288	-9.556	-8.908	-9.325	-9.734	-9.909
50	-9.257	-9.766	-10.918	-11.486	-8.921	-9.070	-9.831	-10.286	-11.486	-10.395	-9.658	-8.983	-9.422	-9.836	-10.013
51	-9.317	-9.846	-10.975	-11.628	-8.983	-9.144	-9.921	-10.393	-11.628	-10.499	-9.756	-9.055	-9.518	-9.921	-10.105
52	-9.370	-9.926	-11.053	-11.770	-9.049	-9.214	-10.017	-10.500	-11.770	-10.610	-9.857	-9.128	-9.618	-10.026	-10.210
53	-9.429	-10.013	-11.169	-11.912	-9.107	-9.289	-10.107	-10.606	-11.912	-10.719	-9.958	-9.197	-9.714	-10.116	-10.307
54	-9.485	-10.091	-11.262	-12.054	-9.164	-9.358	-10.202	-10.716	-12.054	-10.833	-10.052	-9.269	-9.813	-10.206	-10.411
55	-9.527	-10.172	-11.402	-12.196	-9.226	-9.435	-10.290	-10.826	-12.196	-10.947	-10.150	-9.341	-9.912	-10.305	-10.511
56	-9.577	-10.263	-11.492	-12.339	-9.287	-9.502	-10.387	-10.932	-12.339	-11.057	-10.244	-9.404	-10.003	-10.400	-10.605
57	-9.632	-10.321	-11.606	-12.481	-9.337	-9.571	-10.475	-11.042	-12.481	-11.170	-10.338	-9.475	-10.102	-10.483	-10.697
58	-9.666	-10.414	-11.688	-12.623	-9.393	-9.643	-10.564	-11.152	-12.623	-11.280	-10.432	-9.534	-10.192	-10.577	-10.797
59	-9.725	-10.478	-11.782	-12.765	-9.437	-9.705	-10.660	-11.257	-12.765	-11.392	-10.519	-9.605	-10.286	-10.668	-10.890
60	-9.754	-10.559	-11.867	-12.907	-9.496	-9.779	-10.751	-11.365	-12.907	-11.506	-10.606	-9.662	-10.375	-10.755	-10.979
61	-9.814	-10.625	-11.953	-13.050	-9.548	-9.849	-10.841	-11.471	-13.050	-11.613	-10.695	-9.725	-10.459	-10.831	-11.072
62	-9.860	-10.710	-12.148	-13.192	-9.577	-9.910	-10.935	-11.579	-13.192	-11.722	-10.781	-9.786	-10.556	-10.943	-11.166
63	-9.868	-10.757	-12.259	-13.334	-9.641	-9.971	-11.020	-11.684	-13.334	-11.834	-10.860	-9.856	-10.641	-11.045	-11.253
64	-9.930	-10.839	-12.370	-13.476	-9.680	-10.030	-11.109	-11.792	-13.476	-11.940	-10.946	-9.906	-10.727	-11.136	-11.354
65	-9.996	-10.907	-12.481	-13.618	-9.732	-10.082	-11.201	-11.891	-13.618	-12.047	-11.025	-9.962	-10.793	-11.172	-11.418
66	-10.002	-10.971	-12.592	-13.760	-9.787	-10.153	-11.280	-11.998	-13.760	-12.162	-11.107	-10.039	-10.896	-11.322	-11.543
67	-10.057	-11.019	-12.703	-13.903	-9.839	-10.212	-11.378	-12.105	-13.903	-12.266	-11.185	-10.072	-10.964	-11.375	-11.617
68	-10.105	-11.110	-12.814	-14.045	-9.889	-10.281	-11.454	-12.202	-14.045	-12.377	-11.264	-10.131	-11.056	-11.500	-11.715
69	-10.112	-11.151	-12.925	-14.187	-9.924	-10.308	-11.545	-12.311	-14.187	-12.490	-11.334	-10.198	-11.135	-11.589	-11.794
70	-10.172	-11.232	-13.035	-14.329	-9.981	-10.408	-11.639	-12.408	-14.329	-12.604	-11.421	-10.236	-11.207	-11.633	-11.896
71	-10.201	-11.255	-13.146	-14.471	-10.040	-10.411	-11.710	-12.510	-14.471	-12.714	-11.495	-10.312	-11.304	-11.806	-11.994
72	-10.224	-11.351	-13.257	-14.614	-10.073	-10.497	-11.804	-12.607	-14.614	-12.835	-11.559	-10.353	-11.360	-11.870	-12.072

73	-10.283	-11.406	-13.368	-14.756	-10.133	-10.539	-11.877	-12.722	-14.756	-12.948	-11.642	-10.401	-11.440	-11.946	-12.206
74	-10.299	-11.446	-13.479	--	-10.175	-10.586	-11.985	-12.804	--	-13.064	-11.716	-10.488	-11.531	-12.046	-12.273
75	-10.344	-11.534	-13.590	--	-10.229	-10.635	-12.034	-12.920	--	-13.191	-11.786	-10.508	-11.617	-12.183	-12.394
76	-10.341	-11.546	-13.701	--	-10.250	-10.696	-12.138	-13.011	--	-13.323	-11.864	-10.571	-11.669	-12.314	-12.501
77	-10.396	-11.619	-13.812	--	-10.307	-10.726	-12.203	-13.132	--	-13.445	-11.929	-10.603	-11.760	-12.391	-12.641
78	-10.433	-11.681	-13.923	--	-10.360	-10.789	-12.306	-13.235	--	-13.575	-12.002	-10.666	-11.831	-12.516	-12.691
79	-10.469	-11.739	-14.034	--	-10.424	-10.844	-12.348	-13.328	--	-13.734	-12.076	-10.736	-11.928	-12.577	-12.836
80	-10.540	-11.797	-14.144	--	-10.465	-10.899	-12.470	-13.405	--	-13.879	-12.165	-10.779	-11.959	-12.757	-12.914
81	-10.584	-11.854	-14.255	--	-10.491	-10.953	-12.520	-13.516	--	-13.977	-12.211	-10.833	-12.072	-12.820	-13.064
82	-10.531	-11.912	-14.366	--	-10.535	-11.008	-12.631	-13.617	--	-14.105	-12.292	-10.886	-12.199	-13.003	--
83	-10.587	-11.969	-14.477	--	-10.563	-11.062	-12.697	-13.752	--	-14.234	-12.358	-10.939	-12.221	-13.087	--
84	-10.682	-12.027	-14.588	--	-10.591	-11.117	-12.745	-13.788	--	-14.362	-12.449	-10.992	-12.329	-13.246	--
85	-10.709	-12.084	-14.699	--	-10.639	-11.172	-12.829	-13.921	--	-14.490	-12.507	-11.045	-12.365	-13.310	--
86	-10.741	-12.142	-14.810	--	-10.671	-11.226	-12.875	--	--	-14.619	-12.578	-11.098	-12.396	-13.494	--
87	-10.649	-12.199	-14.921	--	-10.710	-11.281	-13.012	--	--	-14.747	-12.659	-11.151	-12.506	-13.724	--
88	-10.692	-12.257	-15.032	--	-10.737	-11.335	-13.141	--	--	-14.876	-12.711	-11.204	-12.627	--	--
89	-10.700	-12.315	-15.143	--	-10.771	-11.390	--	--	--	-15.004	-12.800	-11.257	-12.734	--	--
90	-10.769	-12.372	--	--	-10.813	-11.445	--	--	--	-15.132	-12.871	-11.310	-12.825	--	--
91	-10.838	-12.430	--	--	-10.867	-11.499	--	--	--	-15.261	-12.933	-11.364	-12.977	--	--
92	-10.874	-12.487	--	--	-10.903	-11.554	--	--	--	-15.389	-13.047	-11.417	--	--	--
93	-10.789	-12.545	--	--	-10.936	-11.608	--	--	--	-15.518	-13.096	-11.470	--	--	--
94	-10.901	-12.602	--	--	-10.966	-11.663	--	--	--	-15.646	-13.127	-11.523	--	--	--
95	-10.901	-12.660	--	--	-11.034	-11.718	--	--	--	--	-13.272	-11.576	--	--	--
96	-10.952	-12.717	--	--	-11.081	-11.772	--	--	--	--	-13.301	-11.629	--	--	--
97	-10.955	--	--	--	-11.112	-11.827	--	--	--	--	-13.386	-11.682	--	--	--
98	-11.013	--	--	--	-11.177	-11.881	--	--	--	--	-13.429	-11.735	--	--	--

99	-11.026	--	--	--	-11.187	-11.936	--	--	--	--	-13.520	-11.788	--	--	--
100	-11.038	--	--	--	-11.256	-11.991	--	--	--	--	-13.592	-11.841	--	--	--

360

361

Table S5-3 Extrapolation of the total hydrocarbon distribution for C100+ components (Dashed lines in Fig. 2c)

C number	value	C number	value	C number	value	C number	value
101	-11.2632	117	-11.81959	133	-12.3760	149	-12.93246
102	-11.2979	118	-11.85437	134	-12.4108	150	-12.96724
103	-11.3327	119	-11.88915	135	-12.4456	151	-13.00201
104	-11.3675	120	-11.92393	136	-12.4804	152	-13.03679
105	-11.4023	121	-11.9587	137	-12.5151	153	-13.07157
106	-11.4370	122	-11.99348	138	-12.5499	154	-13.10634
107	-11.4718	123	-12.02826	139	-12.5847	155	-13.14112
108	-11.5066	124	-12.06303	140	-12.6195	156	-13.1759
109	-11.5414	125	-12.09781	141	-12.6542	157	-13.21067
110	-11.5762	126	-12.13259	142	-12.6890	158	-13.24545
111	-11.6109	127	-12.16736	143	-12.7238	159	-13.28023
112	-11.6457	128	-12.20214	144	-12.7586	160	-13.31501
113	-11.6805	129	-12.23692	145	-12.7934	161	-13.34978
114	-11.7153	130	-12.2717	146	-12.8281	162	-13.38456
115	-11.7500	131	-12.30647	147	-12.8629	163	-13.41934
116	-11.78482	132	-12.34125	148	-12.8977	164	-13.45411

362

363

364

Table S5-4 The detailed data of the olefin distribution in Fig. 2c, Fig. 4a2 – Fig. 4d2

C															
Number	R1	R2	R3	R4	HC-1	HC-2	HC-4	HC-5	SV-10	SV-25	SV-60	T-265	T-275	T-285	T-295
1	--	--	--	--	--	--	--	--	--	--	--	--	--	--	--
2	-6.632	-4.669	-4.706	-6.380	-4.782	-4.729	-5.219	-5.317	-6.380	-5.109	-4.700	-4.866	-5.085	-5.200	-5.089
3	-5.046	-4.236	-4.327	-4.818	-4.721	-4.571	-4.757	-4.653	-4.818	-4.400	-4.375	-4.653	-4.755	-4.776	-4.665
4	-5.324	-4.706	-4.551	-5.262	-5.169	-5.043	-4.946	-4.821	-5.262	-4.956	-4.864	-5.088	-5.074	-4.941	-4.834
5	-5.567	-5.096	-4.772	-5.602	-5.544	-5.433	-5.124	-4.996	-5.602	-5.308	-5.228	-5.468	-5.350	-5.114	-5.020
6	-5.608	-5.420	-4.992	-5.883	-5.881	-5.675	-5.366	-5.239	-5.883	-5.583	-5.565	-5.816	-5.568	-5.305	-5.205
7	-5.605	-5.658	-5.198	-6.127	-6.247	-6.081	-5.562	-5.433	-6.127	-5.795	-5.824	-6.104	-5.729	-5.446	-5.368
8	-5.688	-5.879	-5.390	-6.434	-6.399	-6.232	-5.718	-5.603	-6.434	-6.027	-6.024	-6.256	-5.867	-5.565	-5.511
9	-5.824	-6.059	-5.586	-6.661	-6.582	-6.407	-5.896	-5.812	-6.661	-6.260	-6.216	-6.428	-6.024	-5.718	-5.682
10	-5.968	-6.251	-5.796	-6.993	-6.721	-6.549	-6.065	-6.025	-6.993	-6.545	-6.391	-6.564	-6.185	-5.891	-5.853
11	-6.131	-6.466	-6.016	-7.354	-6.875	-6.698	-6.253	-6.258	-7.354	-6.837	-6.609	-6.707	-6.365	-6.059	-6.024
12	-6.316	-6.697	-6.245	-7.752	-7.009	-6.843	-6.455	-6.504	-7.752	-7.207	-6.856	-6.887	-6.578	-6.257	-6.214
13	-6.496	-6.960	-6.516	-8.114	-7.136	-6.994	-6.670	-6.762	-8.114	-7.587	-7.127	-7.073	-6.794	-6.464	-6.464
14	-6.632	-7.122	-6.803	-8.395	-7.261	-7.139	-6.895	-7.022	-8.395	-7.916	-7.372	-7.219	-6.978	-6.612	-6.681
15	-6.786	-7.332	-7.120	-8.716	-7.374	-7.284	-7.125	-7.282	-8.716	-8.300	-7.620	-7.377	-7.174	-6.780	-6.926
16	-6.926	-7.532	-7.426	-8.968	-7.503	-7.435	-7.352	-7.529	-8.968	-8.653	-7.881	-7.527	-7.334	-6.950	-7.143
17	-7.081	-7.794	-7.774	-9.221	-7.634	-7.547	-7.574	-7.785	-9.221	-8.934	-8.110	-7.706	-7.528	-7.159	-7.391
18	-7.255	-8.043	-8.075	-9.639	-7.684	-7.660	-7.792	-8.047	-9.639	-9.261	-8.324	-7.892	-7.715	-7.352	-7.601
19	-7.446	-8.348	-8.391	-9.962	-7.763	-7.833	-8.011	-8.312	-9.962	-9.449	-8.548	-8.097	-7.907	-7.564	-7.818
20	-7.655	-8.664	-8.682	-10.285	-7.841	-7.941	-8.240	-8.583	-10.285	-9.799	-8.847	-8.309	-8.118	-7.787	-8.018
21	-7.877	-8.953	-8.801	-10.609	-7.869	-8.013	-8.393	-8.774	-10.609	-10.082	-9.041	-8.456	-8.299	-7.999	-8.227
22	-8.004	-9.243	-9.106	-10.932	-7.938	-8.137	-8.584	-9.032	-10.932	-10.321	-9.261	-8.609	-8.490	-8.229	-8.428
23	-8.256	-9.526	-9.383	-11.255	-8.009	-8.273	-8.775	-9.317	-11.255	-10.583	-9.476	-8.753	-8.681	-8.447	-8.631

24	-8.631	-9.786	-9.521	-11.579	-8.089	-8.430	-8.999	-9.535	-11.579	-10.844	-9.690	-8.867	-8.872	-8.645	-8.808
25	-9.001	-10.024	-9.675	-11.902	-8.160	-8.579	-9.285	-9.781	-11.902	-11.089	-9.879	-9.003	-9.062	-8.872	-9.031
26	-9.187	-10.244	-10.079	-12.225	-8.268	-8.788	-9.527	-10.151	-12.225	-11.395	-10.061	-9.140	-9.253	-9.096	-9.256
27	-9.321	-10.423	-10.265	-12.549	-8.331	-8.903	-9.739	-10.336	-12.549	-11.667	-10.259	-9.266	-9.444	-9.327	-9.489
28	-9.568	-10.591	-10.465	-12.872	-8.381	-9.076	-9.848	-10.624	-12.872	-11.938	-10.495	-9.404	-9.635	-9.543	-9.744
29	-9.780	-10.803	-10.520	-13.195	-8.461	-9.242	-10.103	-10.853	-13.195	-12.210	-10.708	-9.534	-9.826	-9.779	-9.987
30	-9.948	-11.124	-10.841	-13.519	-8.534	-9.396	-10.322	-11.109	-13.519	-12.481	-10.918	-9.676	-10.017	-10.073	-10.320
31	-10.243	-11.384	-11.071	-13.842	-8.606	-9.470	-10.578	-11.400	-13.842	-12.753	-11.127	-9.810	-10.208	-10.304	-10.534
32	-10.434	-11.476	-11.290	-14.165	-8.672	-9.615	-10.796	-11.678	-14.165	-13.024	-11.337	-9.945	-10.399	-10.535	-10.843
33	-10.725	-11.741	-11.509	-14.488	-8.738	-9.759	-11.015	-11.955	-14.488	-13.296	-11.546	-10.080	-10.589	-10.765	-11.034
34	-10.962	-11.960	-11.727	-14.812	-8.804	-9.903	-11.234	-12.232	-14.812	-13.568	-11.756	-10.215	-10.780	-10.996	-11.209
35	-11.199	-12.178	-11.946	-15.135	-8.870	-10.048	-11.452	-12.509	-15.135	-13.839	-11.965	-10.350	-10.971	-11.227	-11.529
36	-11.435	-12.397	-12.165	-15.458	-8.936	-10.192	-11.671	-12.786	-15.458	-14.111	-12.175	-10.484	-11.162	-11.457	-11.780
37	-11.672	-12.616	-12.384	-15.782	-9.002	-10.337	-11.889	-13.063	-15.782	-14.382	-12.384	-10.619	-11.353	-11.688	-12.032
38	-11.909	-12.834	-12.603	-16.105	-9.068	-10.481	-12.108	-13.340	-16.105	-14.654	-12.594	-10.754	-11.544	-11.919	-12.284
39	-12.145	-13.053	-12.821	-16.428	-9.134	-10.626	-12.327	-13.618	-16.428	-14.925	-12.803	-10.889	-11.735	-12.150	-12.535
40	-12.382	-13.272	-13.040	-16.752	-9.200	-10.770	-12.545	-13.895	-16.752	-15.197	-13.013	-11.024	-11.925	-12.380	-12.787
41	-12.619	-13.490	-13.259	-17.075	-9.265	-10.915	-12.764	-14.172	-17.075	-15.469	-13.222	-11.159	-12.116	-12.611	-13.038
42	-12.856	-13.709	-13.478	-17.398	-9.331	-11.059	-12.983	-14.449	-17.398	-15.740	-13.432	-11.293	-12.307	-12.842	-13.290
43	-13.092	-13.928	-13.697	-17.721	-9.397	-11.203	-13.201	-14.726	-17.721	-16.012	-13.641	-11.428	-12.498	-13.072	-13.542
44	-13.329	-14.146	-13.915	-18.045	-9.463	-11.348	-13.420	-15.003	-18.045	-16.283	-13.851	-11.563	-12.689	-13.303	-13.793
45	-13.566	-14.365	-14.134	-18.368	-9.529	-11.492	-13.638	-15.280	-18.368	-16.555	-14.060	-11.698	-12.880	-13.534	-14.045

366 Note: The olefin distribution of C31~C45 was obtained by extrapolation.

367

368

Table S5-5 The detailed data of the paraffin distribution in Fig. 2c, Fig. 4a3 – Fig. 4d3

C															
Number	R1	R2	R3	R4	HC-1	HC-2	HC-4	HC-5	SV-10	SV-25	SV-60	T-265	T-275	T-285	T-295
1	-3.275	-2.745	-3.073	-2.168	-3.926	-3.439	-3.003	-2.696	-2.168	-2.337	-2.736	-3.475	-3.331	-3.266	-3.030
2	-5.287	-4.899	-5.419	-3.923	-6.180	-5.658	-5.771	-5.465	-3.923	-4.059	-4.832	-5.738	-5.816	-6.150	-5.803
3	-5.849	-5.409	-5.630	-4.807	-6.301	-5.874	-6.017	-5.898	-4.807	-5.072	-5.457	-5.931	-6.075	-6.313	-6.120
4	-6.197	-5.627	-5.666	-5.109	-6.507	-6.114	-5.989	-5.829	-5.109	-5.419	-5.725	-6.131	-6.171	-6.260	-6.080
5	-6.529	-6.013	-5.867	-5.258	-6.796	-6.464	-6.148	-5.970	-5.258	-5.692	-6.070	-6.467	-6.419	-6.402	-6.209
6	-6.713	-6.280	-6.071	-5.434	-6.998	-6.759	-6.331	-6.089	-5.434	-5.832	-6.330	-6.783	-6.564	-6.538	-6.397
7	-6.788	-6.496	-6.261	-5.562	-7.355	-7.043	-6.451	-6.168	-5.562	-5.929	-6.554	-7.005	-6.615	-6.603	-6.509
8	-6.910	-6.672	-6.389	-5.661	-7.565	-7.169	-6.526	-6.210	-5.661	-5.991	-6.652	-7.142	-6.693	-6.696	-6.586
9	-7.012	-6.844	-6.536	-5.787	-7.648	-7.294	-6.609	-6.280	-5.787	-6.091	-6.758	-7.237	-6.786	-6.807	-6.715
10	-7.134	-6.960	-6.661	-5.908	-7.752	-7.388	-6.674	-6.342	-5.908	-6.167	-6.801	-7.280	-6.859	-6.837	-6.760
11	-7.279	-7.055	-6.751	-6.016	-7.863	-7.474	-6.738	-6.409	-6.016	-6.242	-6.810	-7.384	-6.898	-6.869	-6.868
12	-7.362	-7.088	-6.849	-6.119	-7.966	-7.555	-6.806	-6.482	-6.119	-6.304	-6.818	-7.349	-6.918	-6.870	-6.954
13	-7.424	-7.136	-6.928	-6.252	-8.030	-7.615	-6.868	-6.561	-6.252	-6.425	-6.827	-7.379	-6.959	-6.911	-6.975
14	-7.453	-7.213	-6.959	-6.362	-8.095	-7.650	-6.937	-6.642	-6.362	-6.552	-6.856	-7.407	-6.993	-7.005	-7.040
15	-7.435	-7.246	-7.000	-6.473	-8.113	-7.673	-6.982	-6.730	-6.473	-6.711	-6.880	-7.410	-7.031	-7.062	-7.091
16	-7.448	-7.270	-7.054	-6.588	-8.127	-7.673	-7.019	-6.790	-6.588	-6.869	-6.935	-7.422	-7.074	-7.121	-7.176
17	-7.412	-7.266	-7.083	-6.692	-8.170	-7.679	-7.049	-6.856	-6.692	-7.018	-6.994	-7.405	-7.080	-7.140	-7.214
18	-7.410	-7.283	-7.133	-6.799	-8.244	-7.691	-7.101	-6.931	-6.799	-7.138	-7.055	-7.428	-7.114	-7.198	-7.264
19	-7.438	-7.267	-7.152	-6.889	-8.261	-7.708	-7.160	-7.010	-6.889	-7.217	-7.083	-7.431	-7.104	-7.207	-7.294
20	-7.474	-7.313	-7.267	-7.057	-8.282	-7.716	-7.216	-7.143	-7.057	-7.341	-7.150	-7.381	-7.154	-7.271	-7.321
21	-7.497	-7.356	-7.351	-7.226	-8.284	-7.701	-7.277	-7.175	-7.226	-7.438	-7.219	-7.430	-7.194	-7.330	-7.354
22	-7.530	-7.409	-7.447	-7.415	-8.308	-7.734	-7.352	-7.287	-7.415	-7.524	-7.290	-7.447	-7.240	-7.388	-7.395
23	-7.420	-7.475	-7.553	-7.602	-8.317	-7.755	-7.462	-7.422	-7.602	-7.602	-7.367	-7.466	-7.295	-7.453	-7.449

24	-7.475	-7.549	-7.732	-7.768	-8.360	-7.760	-7.537	-7.495	-7.768	-7.683	-7.434	-7.503	-7.348	-7.541	-7.522
25	-7.533	-7.630	-7.842	-7.940	-8.336	-7.774	-7.614	-7.586	-7.940	-7.762	-7.509	-7.539	-7.430	-7.610	-7.588
26	-7.585	-7.713	-8.075	-8.099	-8.337	-7.837	-7.692	-7.712	-8.099	-7.866	-7.590	-7.579	-7.500	-7.688	-7.666
27	-7.646	-7.812	-8.235	-8.244	-8.382	-7.879	-7.751	-7.783	-8.244	-7.969	-7.668	-7.628	-7.570	-7.711	-7.750
28	-7.722	-7.909	-8.367	-8.380	-8.450	-7.928	-7.823	-7.867	-8.380	-8.073	-7.748	-7.681	-7.643	-7.870	-7.843
29	-7.777	-8.002	-8.506	-8.512	-8.487	-7.953	-7.894	-7.992	-8.512	-8.181	-7.831	-7.738	-7.718	-7.960	-7.937
30	-7.835	-8.089	-8.621	-8.645	-8.519	-8.002	-8.006	-8.070	-8.645	-8.292	-7.916	-7.792	-7.794	-8.044	-8.029
31	-7.907	-8.183	-8.735	-8.795	-8.497	-7.990	-8.090	-8.253	-8.795	-8.413	-8.017	-7.855	-7.875	-8.134	-8.141
32	-7.986	-8.270	-8.849	-8.929	-8.531	-8.041	-8.182	-8.360	-8.929	-8.523	-8.100	-7.910	-7.953	-8.223	-8.239
33	-8.068	-8.352	-8.970	-9.068	-8.570	-8.095	-8.273	-8.468	-9.068	-8.631	-8.184	-7.962	-8.029	-8.314	-8.347
34	-8.153	-8.438	-9.089	-9.211	-8.608	-8.150	-8.366	-8.576	-9.211	-8.740	-8.268	-8.018	-8.108	-8.404	-8.460
35	-8.202	-8.524	-9.202	-9.356	-8.650	-8.208	-8.459	-8.683	-9.356	-8.843	-8.351	-8.075	-8.185	-8.497	-8.561
36	-8.274	-8.610	-9.348	-9.501	-8.691	-8.264	-8.555	-8.795	-9.501	-8.950	-8.433	-8.134	-8.259	-8.591	-8.665
37	-8.344	-8.692	-9.394	-9.642	-8.733	-8.322	-8.647	-8.905	-9.642	-9.053	-8.516	-8.193	-8.338	-8.671	-8.774
38	-8.434	-8.780	-9.476	-9.784	-8.772	-8.381	-8.742	-9.014	-9.784	-9.157	-8.597	-8.252	-8.416	-8.766	-8.872
39	-8.488	-8.862	-9.562	-9.923	-8.812	-8.437	-8.837	-9.123	-9.923	-9.260	-8.680	-8.307	-8.497	-8.852	-8.974
40	-8.556	-8.948	-9.663	-10.061	-8.852	-8.494	-8.931	-9.230	-10.061	-9.364	-8.760	-8.363	-8.577	-8.939	-9.070
41	-8.626	-9.029	-9.796	-10.207	-8.889	-8.552	-9.022	-9.338	-10.207	-9.471	-8.842	-8.422	-8.659	-9.022	-9.168
42	-8.699	-9.112	-9.937	-10.349	-8.930	-8.606	-9.114	-9.443	-10.349	-9.576	-8.923	-8.477	-8.737	-9.109	-9.258
43	-8.773	-9.192	-10.071	-10.491	-8.973	-8.665	-9.205	-9.550	-10.491	-9.680	-9.004	-8.537	-8.817	-9.196	-9.352
44	-8.841	-9.271	-10.203	-10.633	-9.016	-8.722	-9.295	-9.654	-10.633	-9.784	-9.090	-8.596	-8.896	-9.281	-9.444
45	-8.915	-9.354	-10.326	-10.775	-9.062	-8.780	-9.387	-9.761	-10.775	-9.886	-9.178	-8.662	-8.984	-9.374	-9.537
46	-8.992	-9.435	-10.439	-10.917	-9.110	-8.841	-9.476	-9.863	-10.917	-9.985	-9.269	-8.729	-9.063	-9.463	-9.628
47	-9.053	-9.516	-10.531	-11.059	-9.163	-8.907	-9.565	-9.970	-11.059	-10.085	-9.365	-8.799	-9.150	-9.557	-9.722
48	-9.130	-9.599	-10.634	-11.201	-9.219	-8.968	-9.655	-10.075	-11.201	-10.187	-9.461	-8.871	-9.245	-9.649	-9.816
49	-9.191	-9.683	-10.747	-11.344	-9.285	-9.039	-9.747	-10.180	-11.344	-10.288	-9.561	-8.944	-9.339	-9.743	-9.914

50	-9.257	-9.769	-10.932	-11.486	-9.345	-9.104	-9.839	-10.289	-11.486	-10.395	-9.662	-9.017	-9.435	-9.844	-10.017
51	-9.317	-9.849	-10.987	-11.628	-9.400	-9.175	-9.928	-10.395	-11.628	-10.499	-9.760	-9.087	-9.529	-9.928	-10.109
52	-9.370	-9.929	-11.063	-11.770	-9.464	-9.242	-10.022	-10.502	-11.770	-10.610	-9.861	-9.159	-9.628	-10.032	-10.213
53	-9.429	-10.015	-11.178	-11.912	-9.513	-9.315	-10.112	-10.607	-11.912	-10.720	-9.962	-9.225	-9.724	-10.121	-10.310
54	-9.485	-10.093	-11.270	-12.054	-9.562	-9.382	-10.206	-10.717	-12.054	-10.833	-10.055	-9.296	-9.822	-10.210	-10.413
55	-9.527	-10.173	-11.409	-12.197	-9.619	-9.457	-10.294	-10.827	-12.197	-10.947	-10.152	-9.366	-9.919	-10.308	-10.513
56	-9.577	-10.264	-11.499	-12.339	-9.674	-9.522	-10.391	-10.934	-12.339	-11.058	-10.246	-9.427	-10.009	-10.404	-10.606
57	-9.632	-10.322	-11.612	-12.481	-9.714	-9.589	-10.478	-11.043	-12.481	-11.170	-10.340	-9.497	-10.108	-10.486	-10.698
58	-9.666	-10.415	-11.693	-12.623	-9.763	-9.660	-10.567	-11.152	-12.623	-11.280	-10.434	-9.555	-10.197	-10.580	-10.798
59	-9.725	-10.479	-11.787	-12.765	-9.795	-9.720	-10.663	-11.258	-12.765	-11.392	-10.520	-9.623	-10.291	-10.670	-10.891
60	-9.754	-10.560	-11.871	-12.907	-9.847	-9.794	-10.753	-11.365	-12.907	-11.506	-10.607	-9.679	-10.380	-10.757	-10.980
61	-9.814	-10.626	-11.956	-13.050	-9.891	-9.862	-10.843	-11.471	-13.050	-11.613	-10.696	-9.742	-10.463	-10.832	-11.073
62	-9.860	-10.710	-12.152	-13.192	-9.902	-9.922	-10.937	-11.580	-13.192	-11.722	-10.782	-9.801	-10.561	-10.945	-11.166
63	-9.868	-10.758	-12.262	-13.334	-9.964	-9.982	-11.021	-11.684	-13.334	-11.834	-10.861	-9.870	-10.645	-11.047	-11.253
64	-9.930	-10.840	-12.373	-13.476	-9.990	-10.040	-11.111	-11.792	-13.476	-11.941	-10.947	-9.919	-10.732	-11.137	-11.354
65	-9.996	-10.907	-12.483	-13.618	-10.034	-10.091	-11.203	-11.891	-13.618	-12.047	-11.026	-9.974	-10.798	-11.173	-11.418
66	-10.002	-10.972	-12.594	-13.760	-10.083	-10.162	-11.281	-11.998	-13.760	-12.163	-11.107	-10.050	-10.900	-11.323	-11.543
67	-10.057	-11.019	-12.705	-13.903	-10.128	-10.220	-11.379	-12.105	-13.903	-12.266	-11.186	-10.082	-10.967	-11.376	-11.617
68	-10.105	-11.110	-12.815	-14.045	-10.171	-10.288	-11.455	-12.203	-14.045	-12.377	-11.264	-10.140	-11.058	-11.501	-11.715
69	-10.112	-11.151	-12.926	-14.187	-10.194	-10.314	-11.546	-12.311	-14.187	-12.490	-11.335	-10.207	-11.136	-11.589	-11.794
70	-10.172	-11.232	-13.037	-14.329	-10.247	-10.413	-11.640	-12.408	-14.329	-12.604	-11.421	-10.244	-11.207	-11.634	-11.896
71	-10.201	-11.255	-13.148	-14.471	-10.301	-10.416	-11.710	-12.511	-14.471	-12.714	-11.495	-10.319	-11.307	-11.806	-11.994
72	-10.224	-11.351	-13.258	-14.614	-10.322	-10.502	-11.805	-12.608	-14.614	-12.835	-11.559	-10.360	-11.357	-11.871	-12.072
73	-10.283	-11.406	-13.369	-14.756	-10.379	-10.543	-11.877	-12.722	-14.756	-12.948	-11.642	-10.408	-11.437	-11.946	-12.206
74	-10.299	-11.446	-13.480	--	-10.413	-10.589	-11.985	-12.804	--	-13.064	-11.717	-10.494	-11.532	-12.046	-12.273
75	-10.344	-11.534	-13.591	--	-10.462	-10.637	-12.035	-12.920	--	-13.191	-11.786	-10.513	-11.618	-12.183	-12.394

76	-10.341	-11.546	-13.702	--	-10.470	-10.698	-12.138	-13.011	--	-13.323	-11.864	-10.576	-11.669	-12.314	-12.501
77	-10.396	-11.619	-13.812	--	-10.522	-10.727	-12.203	-13.132	--	-13.445	-11.929	-10.608	-11.761	-12.391	-12.641
78	-10.433	-11.682	-13.923	--	-10.572	-10.791	-12.306	-13.235	--	-13.575	-12.002	-10.670	-11.831	-12.516	-12.691
79	-10.469	-11.739	-14.034	--	-10.634	-10.845	-12.348	-13.328	--	-13.734	-12.076	-10.740	-11.929	-12.577	-12.836
80	-10.540	-11.797	-14.145	--	-10.667	-10.900	-12.471	-13.405	--	-13.879	-12.165	-10.783	-11.960	-12.757	-12.914
81	-10.584	-11.854	-14.256	--	-10.683	-10.954	-12.520	-13.516	--	-13.977	-12.211	-10.836	-12.072	-12.820	-13.064
82	-10.531	-11.912	-14.367	--	-10.721	-11.009	-12.631	-13.617	--	-14.105	-12.292	-10.889	-12.144	-13.003	--
83	-10.587	-11.969	-14.477	--	-10.740	-11.063	-12.697	-13.752	--	-14.234	-12.358	-10.942	-12.221	-13.087	--
84	-10.682	-12.027	-14.588	--	-10.759	-11.118	-12.745	-13.788	--	-14.362	-12.449	-10.994	-12.299	-13.246	--
85	-10.709	-12.084	-14.699	--	-10.803	-11.172	-12.829	-13.921	--	-14.490	-12.507	-11.047	-12.365	-13.310	--
86	-10.741	-12.142	-14.810	--	-10.828	-11.227	-12.875	--	--	-14.619	-12.578	-11.100	-12.396	-13.494	--
87	-10.649	-12.199	-14.921	--	-10.862	-11.281	-13.012	--	--	-14.747	-12.659	-11.153	-12.506	-13.724	--
88	-10.692	-12.257	-15.032	--	-10.881	-11.336	-13.142	--	--	-14.876	-12.711	-11.206	-12.627	--	--
89	-10.700	-12.315	-15.143	--	-10.910	-11.390	--	--	--	-15.004	-12.800	-11.259	-12.734	--	--
90	-10.769	-12.372	-15.254	--	-10.947	-11.445	--	--	--	-15.132	-12.871	-11.312	-12.825	--	--
91	-10.838	-12.430	--	--	-10.998	-11.499	--	--	--	-15.261	-12.933	-11.365	-12.977	--	--
92	-10.874	-12.487	--	--	-11.029	-11.554	--	--	--	-15.389	-13.047	-11.418	--	--	--
93	-10.789	-12.545	--	--	-11.057	-11.609	--	--	--	-15.518	-13.096	-11.471	--	--	--
94	-10.901	-12.602	--	--	-11.081	-11.663	--	--	--	-15.646	-13.127	-11.524	--	--	--
95	-10.901	-12.660	--	--	-11.149	-11.718	--	--	--	--	-13.272	-11.577	--	--	--
96	-10.952	-12.717	--	--	-11.193	-11.772	--	--	--	--	-13.301	-11.630	--	--	--
97	-10.955	--	--	--	-11.219	-11.827	--	--	--	--	-13.386	-11.683	--	--	--
98	-11.013	--	--	--	-11.284	-11.882	--	--	--	--	-13.429	-11.736	--	--	--
99	-11.026	--	--	--	-11.287	-11.936	--	--	--	--	-13.520	-11.789	--	--	--
100	-11.038	--	--	--	-11.355	-11.991	--	--	--	--	-13.592	-11.842	--	--	--

References

1. D. L. King, J. A. Cusumano and R. L. Garten, *Catal. Rev.*, 1981, 23, 233-263.
2. E. Iglesia, S. C. Reyes and R. J. Madon, *J. Catal.*, 1991, 129, 238-256.
3. T. Olewski, B. Todic, L. Nowicki, N. Nikacevic and D. B. Bukur, *Chem. Eng. Res. Des.*, 2015, 95, 1-11.
4. G. P. van der Laan and A. Beenackers, *Ind. Eng. Chem. Res.*, 1999, 38, 1277-1290.
5. B. Todic, T. Bhatelia, G. F. Froment, W. Ma, G. Jacobs, B. H. Davis and D. B. Bukur, *Ind. Eng. Chem. Res.*, 2013, 52, 669-679.
6. C. G. Visconti, E. Tronconi, L. Lietti, R. Zennaro and P. Forzatti, *Chem. Eng. Sci.*, 2007, 62, 5338-5343.
7. J. Gaube and H. F. Klein, *J. Mol. Catal. A: Chem.*, 2008, 283, 60-68.
8. C. M. Masuku, D. Hildebrandt and D. Glasser, *Chem. Eng. Sci.*, 2011, 66, 6254-6263.
9. H. G. Stenger Jr, *J. Catal.*, 1985, 92, 426-428.